High-Resolution Solution Structure of a Designed Peptide Bound to Lipopolysaccharide: Transferred Nuclear Overhauser Effects, Micelle Selectivity, and Anti-Endotoxic Activity[†,‡]

Surajit Bhattacharjya,*[,§] Prerna N. Domadia,[§] Anirban Bhunia,[§] Subbalakshmi Malladi,[||] and Sunil A. David[||]

Biomolecular NMR and Drug Discovery Laboratory, School of Biological Sciences, Division of Structural and Computational Biology, Nanyang Technological University, Singapore 637551, and Department of Medicinal Chemistry, University of Kansas, Multidisciplinary Research Building, Room 320D, 2030 Becker Drive, Lawrence Kansas 66047

Received December 5, 2006; Revised Manuscript Received February 27, 2007

ABSTRACT: Designing peptides that would interact with lipopolysaccharides (LPS) and acquire a specific folded conformation can generate useful structural insights toward the development of anti-sepsis agents. In this work, we have constructed a 12-residue linear peptide, YW12, rich in aromatic and aliphatic amino acid residues with a centrally located stretch of four consecutive positively charged (KRKR) residues. In absence of LPS, YW12 is predominantly unstructured in aqueous solution. Using transferred nuclear Overhauser effect (Tr-NOE) spectroscopy, we demonstrate that YW12 adopts a well-folded structure as a complex with LPS. Structure calculations reveal that YW12 assumes an extended conformation at the N-terminus followed by two consecutive β-turns at its C-terminus. A hydrophobic core is formed by extensive packing between number of aromatic and nonpolar residues, whereas the positively charged residues are segregated out to a separate region essentially stabilizing an amphipathic structure. In an *in vitro* LPS neutralization assay using NF-κB induction as the readout, YW12 shows moderate activity with an IC_{50} value of $\sim$10 μM. As would be expected, tryptophan fluorescence studies demonstrate that YW12 shows selective interactions only with the negatively charged lipid micelles including sodium dodecyl sulfate (SDS), 1-palmitoyl-2-oleoylphosphatidyl-DL-glycerol (POPG), and LPS, and no significant interactions are detected with zwitterionic lipid micelles such as dodecyl-phosphocholine (DPC). Far-UV CD studies indicate the presence of β-turns or β-sheet-like conformations of the peptide in negatively charged micelles, whereas no structural transitions are apparent in DPC micelles. These results suggest that structural features of YW12 could be utilized to develop nontoxic antisepsis compounds.

Lipopolysaccharide (LPS)[1], also called endotoxin, is a major constituent of the outer membrane of Gram negative bacteria (*1*). LPS is released into systemic circulation, either because of invasion of Gram negative bacteria or as a consequence of intensive antimicrobial chemotherapy of severe microbial infections (*2*, *3*). Circulating LPS in the blood stream is recognized by the phagocytic cells, monocytes, and macrophages of the innate immune system of the host. Once induced by LPS, these phagocytes secrete proinflammatory cytokines, important among which are tumor necrosis factor-α (TNF-α), interleukin-6 (IL-6), and interleukin-1β (IL-1β) (*4*−*6*). The release of cytokines in response to pathogenic invasion is a natural function of innate immune defense. However, an uncontrolled and overwhelming production of these cytokines may lead to constellation of symptoms termed endotoxic shock or septic shock, characterized by endothelial damage, loss of vascular tone, coagulopathy, and multiple system organ failure, frequently resulting in death (*7*, *8*). LPS mediated activation of macrophages and concomitant overproduction of tissue-damaging cytokines are a complex cascade of events. At the molecular level, LPS, upon release into blood, is recognized by a serum protein called lipopolysaccharide binding protein or LBP. The LBP/LPS complex interacts with a receptor, CD14, at the surface of the macrophage (*9*, *10*). The ternary complex (LBP/LPS/CD14) activates a Toll-like pattern recognition receptor (TLR4) that in turn initiates parallel signaling cascades resulting in over production of inflammatory cytokines and reactive oxygen species (*11*, *12*). Septic shock is the major cause of mortality in the intensive care unit accounting for 600,000 deaths every year in the United States alone (*13*). A potential strategy to overcome sepsis mediated lethality would be the discovery and development

[†] This work was funded by a research grant (SBS/SUG/34/06) from the School of Biological Sciences, Nanyang Technological University to S.B., and S.D. was funded by NIH grants 1R01 AI50107 and 1U01 AI056476.

[‡] The coordinates of LPS bound YW12 structures have been deposited in the Protein Data Bank (file name 2OoS). The chemical shift values are deposited in the BioMagResBank (accession number: 15118).

* To whom correspondence should be addressed. Phone: +65-6316-7997. Fax: +65-6791-3856. E-mail: surajit@ntu.edu.sg.

[§] Nanyang Technological University.

[||] University of Kansas.

[1] Abbreviations: LPS, lipopolysaccharide; NMR, nuclear magnetic resonance; Tr-NOE, transferred nuclear Overhauser effect; Et-NOE, exchanged transferred nuclear Overhauser effect; NOESY, nuclear Overhauser effect spectroscopy; TOCSY, total correlation spectroscopy; SDS, sodium dodecyl sulfate; DPC, dodecylphosphocholine; POPG, 1-palmitoyl-2-oleoylphosphatidyl-DL-glycerol; CD, circular dichroism; NOE, nuclear Overhauser enhancement.

10.1021/bi6025159 CCC: $37.00
Published on Web 05/01/2007

of compounds that would bind and sequester LPS, thereby blocking its interactions with the serum and cellular receptors (*14*). LPS binding has been reported for some of the naturally occurring antimicrobial peptides (*15*, *16*), synthetic amphipathic peptides (*17*−*19*), and fragments of LPS binding proteins (*20*, *21*). However, many of these peptides also exert toxic effects and therefore are not suitable for clinical use. For instance, the neurotoxicity and nephrotoxicity of polymyxin B, a cyclic cationic decapeptide highly efficient in detoxifying LPS, limit its application to topical use (*22*). Designing synthetic peptides and determining the three-dimensional structure of peptides in complex with LPS could provide valuable insights for the development of nontoxic anti-sepsis compounds. However, the determination of structure at atomic resolution in complex with LPS remains a difficult problem because of the aggregation and precipitation of peptides in the presence of LPS (*23*). In this work, we have determined the solution conformation of a *de novo* designed 12-residue peptide, YW12, in complex with LPS by using transferred nuclear Overhauser effect (Tr-NOE), also termed exchange transferred nuclear Overhauser effect (Et-NOE), spectroscopy (*24*, *25*). In aqueous solution, free peptide, YW12, exists in a random coil/disordered state but undergoes a dramatic structural stabilization as a complex with LPS. The ensemble of LPS bound conformations of YW12 derived from Tr-NOE constrains is well converged with rmsd of 0.2 and 1.2 Å for backbone atoms and all heavy atoms, respectively. Furthermore, this peptide shows considerable neutralization potency toward LPS. These results could serve as a starting point for the rational design of novel antisepsis agents.

MATERIALS AND METHODS

DPC and POPG were obtained from Avanti Polar Lipids (Alabaster, AL). SDS and LPS were obtained from Sigma (St. Louis, MO).

Synthesis of Peptide. YW12 (NH_2-YVLWKRKRMIFI-COOH) was synthesized by standard F-moc solid-phase peptide synthesis method and purified by reversed-phase HPLC. The molecular weight of the peptide was confirmed by mass spectrometry.

NMR Spectroscopy. All of the NMR experiments were carried out on a Bruker DRX 700 or Bruker DRX 600 spectrometer, equipped with cryo-probe and pulse field gradients. Two-dimensional (2D) ^{1}H-^{1}H TOCSY and ^{1}H-^{1}H NOESY spectra were acquired at 70 and 300 ms mixing times, respectively, for ~1.0 mM free peptide, dissolved in an aqueous solution containing 10% D_2O at pH 4.8. Series of one-dimensional (1D) proton NMR spectra of YW12, with a peptide concentration of 0.8 mM, were collected at various concentrations of LPS ranging from 0.4, 0.8, and 1.6 mg/mL. Because the polysaccharide moiety of LPS is considerably heterogeneous (*1*), concentrations of LPS are given in mass/unit volume. Two-dimensional ^{1}H-^{1}H Tr-NOE (*24*, *25*) spectra were acquired at a peptide/LPS mixture containing 1 mM YW12 peptide and 0.8 mg/mL of LPS at four different mixing times: 250, 200, 150, and 100 ms. At this concentration of LPS (0.8 mg/mL), the peptide/LPS complex appears to be stable over the period of NMR data collection and also generates a large number of Tr-NOE cross-peaks. At higher LPS concentrations, the peptide/LPS complex showed a tendency toward precipitation with increased broadening of NMR resonances. All experiments were performed at a temperature of 290 K and pH 4.8 in an aqueous solution. Tr-NOE experiments were also carried out at pH 6.0; however, extensive broadening of NMR resonances in the presence of LPS precludes sequence specific resonance assignments under such conditions. NMR data processing and analyses were carried out by Topspin (Bruker) and Sparky (Goddard, T. D., and Kneller, D. G., University of California, San Francisco), respectively.

Tr-NOE Driven Structure Calculations of YW12. Structure calculations were carried out by using the DYANA program, version 1.5 (*26*). Structures were calculated solely on the basis of the Tr-NOE driven distance restraints obtained from a Tr-NOESY spectrum recorded at 150 ms mixing time. Calculations of NOE build up rate as a function of mixing time indicate that spin diffusion does not contribute to the observed NOE intensities at 150 ms of mixing time (Figure 1 in the Supporting Information). Dihedral angles or hydrogen bond constraints were not used during structure calculations. The ϕ dihedral angles were constrained between −30° to −180° to maintain good stereochemistry of the calculated structures. NOE intensities were qualitatively categorized to strong, medium, and weak and translated to upper bound distance limits to 2.5, 3.5, and 5.0 Å, respectively. Several rounds of structure calculations were carried out, and depending on NOE violations, distance constraints were adjusted. Of the 100 structures that were generated, 20 lowest energy structures were kept for analyses. In order to judge the convergence of the calculated structures, angular order parameters (S) for the backbone dihedral angles (ϕ, ψ) were estimated using the following equation: $S = 1/N\{(\Sigma \cos \alpha_{k\ (k = 1\ \text{to}\ N)})^2 + (\Sigma \sin \alpha_{k\ (k = 1\ \text{to}\ N)})^2\}$, where α is ϕ or ψ, N represents the total number of lowest energy structures, and k is 1 to N (*27*). S can assume a value between 0 and 1, with $S = 1$ when ϕ or ψ has same value in all of the structures, whereas $S = 0$ is indicative of the random distribution of dihedral angles.

Docking of Peptide to LPS. The Tr-NOE derived structure of YW12 was docked on to LPS by the program AutoDock (*28*). The atomic coordinate of LPS (1QFG), was obtained from the cocrystal structure of LPS and Fhu A (*29*). Grid maps or affinity maps representing LPS were constructed using 70 × 80 × 80 points, with a grid spacing of 0.375 Å, centered at the H2 atom of the glucosamine II residue of the lipid moiety. During docking, the peptide YW12 was used as ligand, and the peptide backbone was kept rigid, while all of the side chains were defined as flexible. LPS−YW12 complexes were generated from this starting point using a Lamarckian genetic algorithm (LGA) with a translation step of 0.2 Å, a quaternion step of 5 Å, and a torsion step (tstep) of 5 Å. The number of individuals in the population changed to 500, and the maximum number of energy evaluations increased to 15,000,000. One hundred LGA docking runs were performed. A total of 100 possible binding conformations were generated and grouped into clusters based on a 1.0 Å cluster tolerance.

Fluorescence Experiments. The intrinsic tryptophan fluorescence spectra of the peptide were acquired using a Cary Eclipse fluorescence spectrophotometer (Varian, Inc.) equipped with dual monochromators. The bandwidths for excitation and emission were 5 and 10 nm, respectively. Measurements

were made using a 0.1 cm path length quartz cuvette. Samples were excited at 295 nm, and emissions were measured between the 300 and 400 nm range. All fluorescence experiments were performed in 10 mM sodium phosphate buffer at a peptide concentration of 5 μM and pH 6.0. Fluorescence emission spectra of YW12 were recorded as a function of the concentration of lipids (LPS, SDS, POPG, and DPC). Fluorescence quenching experiments were performed by stepwise addition of either acrylamide or KI from a stock solution of 5 M into solution containing 5 μM peptide and saturating concentration of lipid micelles, that is, 1.2 mM DPC, 1.2 mM POPG, 10 mM SDS, and 40 μg/mL LPS. Diminution of fluorescence intensities were measured at corresponding emission maxima of the peptide or peptide/lipid complex. The results of the quenching reactions were analyzed according to the Stern−Volmer equation, $F_0/F = 1 + K_{SV}[Q]$, where, F_0 and F are the fluorescence intensities at appropriate emission wavelengths in the absence and presence of quencher, respectively, K_{SV} is the Stern−Volmer quenching constant, and [Q] is the molar quencher concentration.

Circular Dichroism Measurements. CD measurements of YW12 were carried out at a concentration of 10 μM in 10 mM phosphate buffer at pH 6.0, at 20 °C, either in the absence or presence of 1.2 mM DPC, 1.2 mM POPG, and 10.0 mM SDS. Measurements were performed using a Chirascan Circular Dichroism spectrometer (Applied Photophysics Ltd., UK). Each CD spectrum reflects an average of three spectra per measurement. Baseline correction was applied to each spectrum by subtracting from a blank spectrum of a sample containing all components except peptide. The far-UV spectra were collected over the range of 190−230 nm using a 0.01 cm path length sandwich cuvette. A spectral bandwidth of 1 nm and a time constant of 1 s were used for all the measurements to improve the signal-to-noise ratio. CD ellipticity is expressed as molar ellipticity (θ_m) in deg cm^2 dmol^{-1}.

In Vitro Assay for Quantifying LPS Sequestration by YW12. The inhibition of induction of NF-κB (a key transcriptional activator of the innate immune system) was quantified using human embryonic kidney 293 cells cotransfected with TLR4 (LPS receptor), CD14, and MD2 (coreceptors), available from InvivoGen, Inc. (HEK-Blue, San Diego, CA), as per protocols provided by the vendor. Stable expression of secreted alkaline phosphatase (seAP) under control of NF-κB/AP-1 promoters is inducible by LPS and extracellular seAP in the supernatant is proportional to NF-κB induction. seAP was assayed spectrophotometrically using an alkaline phosphatase specific chromogen at 620 nm using a rapid throughput, automated protocol employing a Bio-Tek P2000 liquid handler.

RESULTS

Design of the YW12 Peptide. The construction of the primary amino acid sequence of the YW12 peptide, YVLWKRKRMIFI, is guided by the cocrystal structure of FhuA, a β-barrel outer membrane protein of *E. coli*, with LPS, the only structure available for a protein−LPS complex (*29*). The interfacial residues of FhuA making contacts with LPS are largely distributed over a number of discontinuous β-strand segments of the polypeptide chain (*29*). Therefore, we have considered residues of FhuA that have intimate contacts (interatomic distance ≤ 4.0 Å) with the conserved lipid A moiety of LPS (Figure 1). It is to be noted that the lipid A moiety is the toxic core of LPS (*30*), and hence, residues favorably interacting with lipid A may generate LPS binding or neutralizing peptide. The crystal structure of the FhuA/LPS complex shows that the bis-phosphate groups of lipid A are involved in multiple hydrogen bonds and salt bridge interactions with a group of four positively charged residues, K439, K441, R384, and K357 of FhuA (Figure 1). Interestingly, a structure based alignment, using FhuA as a template, had previously found four basic residues consisting either of Arg and/or Lys in the LPS binding regions from other LPS-interacting proteins (*31*). This observation had led to the proposal of a plausible conserved LPS binding motif that may consist of four positively charged residues (*31*). Taken together, the four basic residues, K5-R6-K7-R8 in the YW12 sequence, correspond to these four positively charged residues of FhuA that may form a LPS binding motif. Because of the potential importance of ionic and hydrogen bond interactions in the stabilization of peptide/LPS complexes (*14*, *20*), these residues are placed at the center of the 12-residue sequence of YW12. We envision that stabilization of the central segment of the peptide on the negatively charged surface of LPS may facilitate further insertion of hydrophobic residues located at the termini of the peptide into the nonpolar core of LPS micelles.

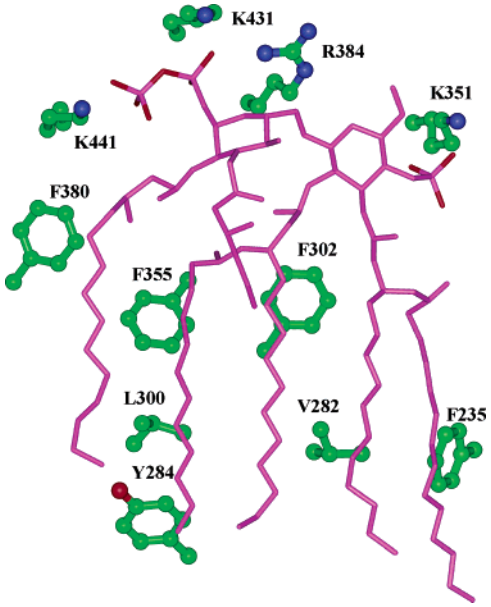

FIGURE 1: Ball and stick representation of the side chains of interfacial residues of FhuA involved in interactions with the lipid A moiety of LPS in the cocrystal structure of the FhuA/LPS complex. The lipid A moiety of LPS is shown in purple. The oxygen atoms of the phosphate groups of lipid A and the hydroxyl oxygen atom of the interfacial residue Y284 of FhuA are shown in red. All nitrogen atoms and all carbon atoms of the side chains of FhuA are depicted in blue and green, respectively. The coordinate set 1QFG (*29*) from the Protein Data Bank was used to generate the diagram.

Apart from ionic and polar interactions, the crystal structure of FhuA/LPS reveals van der Waals contacts (interatomic distance ≤ 4.0 Å) between a number of aromatic and nonpolar residues with the acyl chains of the LPS molecule (Figure 1). These residues are further divided into

two clusters depending on their location on the fatty acyl chains of LPS. Amino acid residues Y284, L300, V282, and F235 of FhuA have packing interactions against the lower part of the alkyl chains of LPS, whereas residues F302, F355, and F380 of FhuA are in contact with the upper part of the alkyl chains of the LPS molecule (Figure 1). Within each cluster, there are residues that have nonbonded contacts (interatomic distance ≤ 4.0 Å) mediated by the side chains, for example, residues Y284 and V282 have van der Waals interactions with residues L300 and F235, respectively. The first four residues, Y1-V2-L3-W4, at the N-terminus of the YW12 sequence correspond to the interfacial residues Y284, V282, L300, and F235 of FhuA, respectively (Figure 1). In order to incorporate a fluorescence probe, the amino acid Trp is selected over Phe. In particular, the N-terminal segment of the YW12 peptide is designed to mimic a native-like packing between residues Y1 (Y284) and L3 (L300), and residues V2 (V282) and W4 (F235), which would persist in a β-sheet-like conformation of the peptide. The high-affinity interactions of FhuA with LPS may have been rendered by its extensive β-sheet structures in the native state (*29*). Furthermore, we have positioned this segment, Y1-V2-L3-W4, at the N-terminus of YW12 in order to place residue W4 in close proximity to the central positively charged cluster because Trp has often been observed adjacent to the positively charged residues in amino acid sequences of membrane active antimicrobial peptides (*32*). At the C-terminus of YW12, three hydrophobic amino acid residues, I10-F11-I12, are selected on the basis of the mutually interacting interfacial residues F302, F355, and F380 of FhuA (Figure 1). In order to enhance the β-sheet forming propensity of the designed sequence, two phenylalanine residues are replaced by the β-branched residue isoleucine. It is noteworthy that Ile has a higher propensity for β-sheet conformations as compared to Phe in a membrane environment (*33*). A Met residue at position 9 is incorporated to help in unambiguous analysis of NMR spectra (*vide infra*), in view of the fact that side chain proton resonances, in particular $C^{\gamma}H_2$ and $C^{\epsilon}H_3$ groups, of Met have unique chemical shift values (*34*). In addition, Met has also been found in membrane active antimicrobial peptides, indicating its possible role in interactions with lipids (*35*).

LPS Neutralization Activity of YW12. We quantified the LPS-neutralizing activity of YW12 using the inhibition of the nuclear translocation of NF-kB as the readout. NF-kB is a key transcriptional activator of the innate immune system, activating cytokine release that ultimately leads to multiple organ failure and the shock syndrome. In this assay, the 50% inhibitory concentration (IC_{50}) of YW12 was found to be 10 μM by standard four-parameter logistic fit (Figure 2), while that of polymyxin B, used as a reference compound, was 1.23 μM (data not shown). Furthermore, we verified that the inhibitory activity was a specific consequence of LPS sequestration because the peptide had no effect on NF-κB induction stimulated by non-LPS stimuli such as TNF-α and phorbol esters (data not shown).

NMR Studies of YW12 in Free and in LPS Bound States. The solution conformation of free YW12 was examined using 2D ^{1}H-^{1}H nuclear Overhauser effect spectroscopy (NOESY) and total correlation spectroscopy (TOCSY). Sequence specific resonance assignments for all the amino

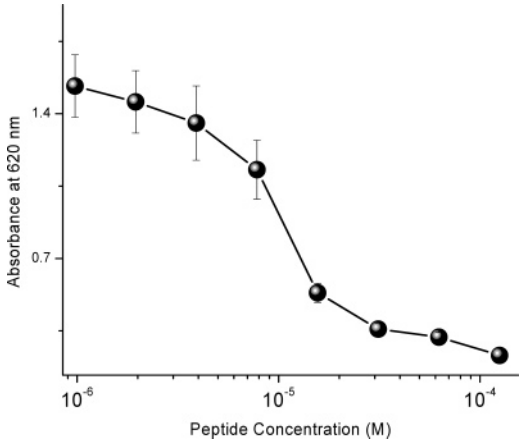

FIGURE 2: Inhibition of NF-kB reporter gene induction in HEK-293 cells stably transfected with the Tlr-4/CD-14/MD-2/NF-kB-SEAP construct. In a 384-well plate, 105 cells per well were stimulated with LPS (10 ng/mL) and exposed to graded concentrations of YW12. Alkaline phosphatase activity was spectrophotometrically quantitated after 12 h at 600 nm using a chromogenic substrate (Invivogen, Inc.). The IC_{50} of YW12 was computed to be 10 μM by four-parameter logistic curve fitting.

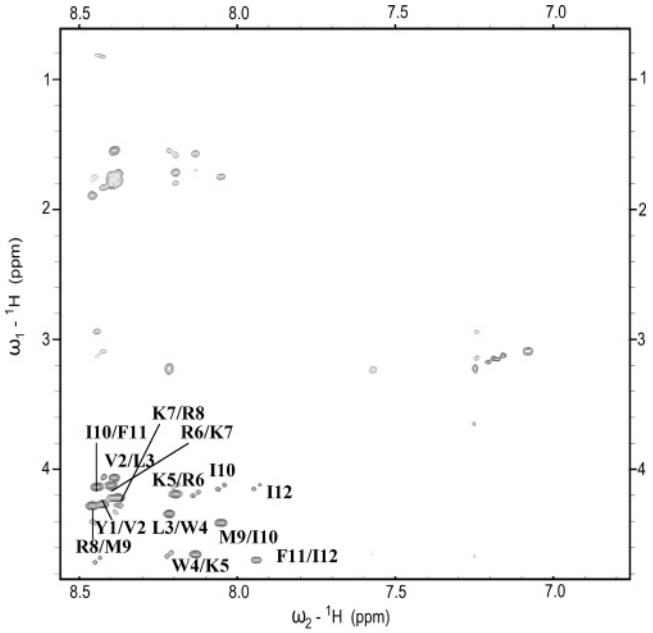

FIGURE 3: Two-dimensional ^{1}H-^{1}H NOESY spectrum of YW12 showing NOEs correlating low-field resonances along the ω_2 dimension and high-field resonances along the ω_1 dimension. The sequential NOEs between backbone resonances are marked.

acids are achieved by combined analyses of TOCSY and NOESY spectra (*34*) (Figure 3). The NOESY spectra of the free peptide are predominantly characterized by weak intra-residue and sequential ($C^{\alpha}H_i/NH_{i+1}$) NOEs between backbone proton resonances (Figure 3). There are very few NOEs correlating backbone to side chain and among side chain resonances that are particularly notable for the aromatic ring protons resonating at 6.8−7.5 ppm. The lack of diagnostic NOEs clearly indicates that the structure of free YW12 is highly dynamic and does not adopt any preferred conformation. In order to confirm that the paucity of NOEs was not due to an unfavorable correlation time ($\omega\tau_c \sim 1.0$) of the molecule, a 2D rotating frame Overhauser effect spectroscopy (ROESY) experiment was carried out. There were no additional medium-range or long-range NOEs in the ROESY

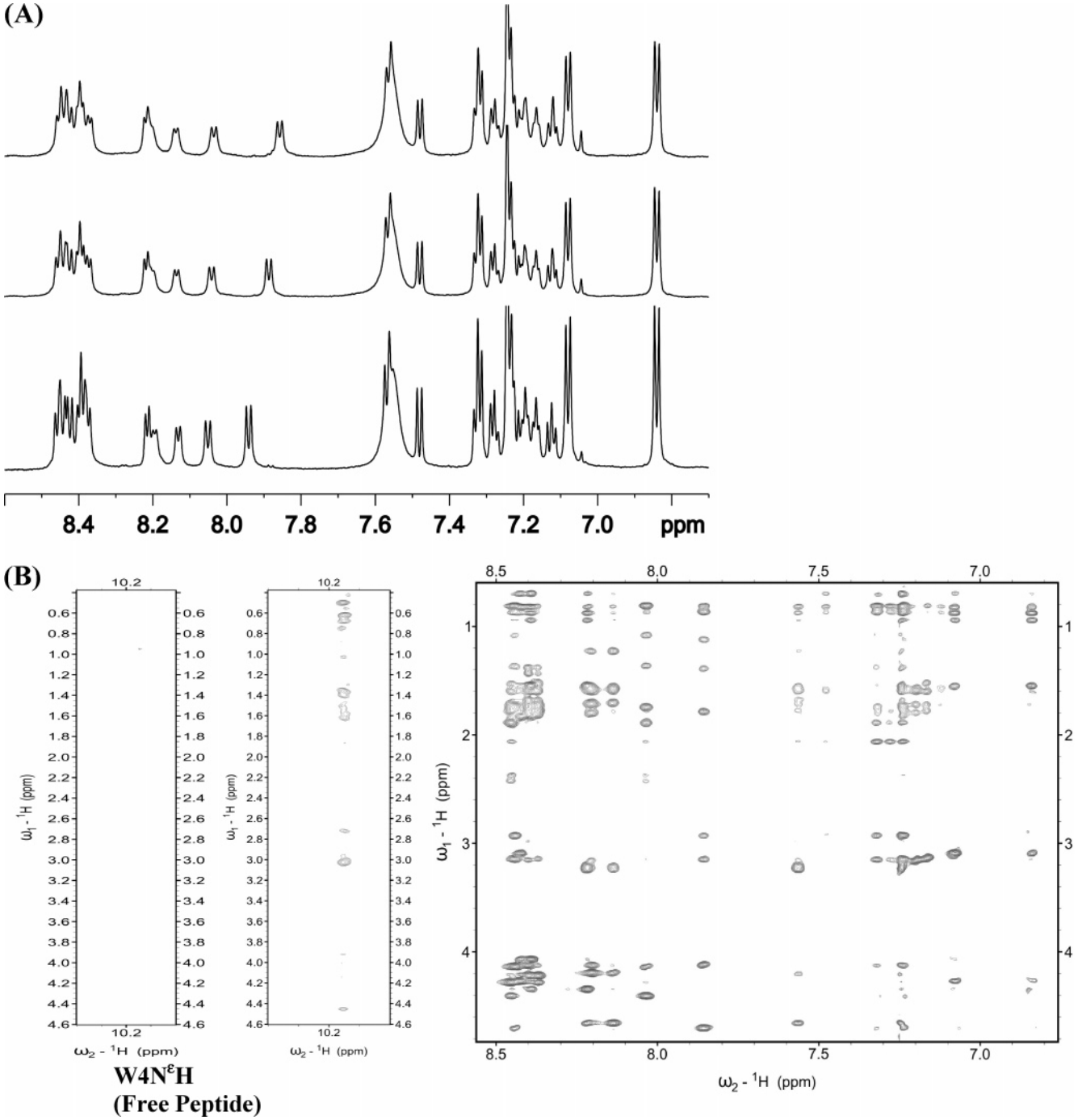

FIGURE 4: (Panel A) Low-field region of the 1D proton NMR spectra of YW12 as a function of concentrations of LPS: 0 mg/mL (bottom), 0.4 mg/mL (middle), and 0.8 mg/mL (top). An upfield shift of the amide proton resonance of the last residue, I12, is observed possibly because of a slight change in pH during LPS titration (panel A). (Panel B) Two-dimensional ^{1}H-^{1}H Tr-NOESY spectra of YW12 showing NOEs correlating low-field resonances along the ω_2 dimension and high-field resonances along the ω_1 dimension. Tr-NOEs (panel B, right) involving the W4 N$^{\varepsilon}$H proton is compared with that of free YW12. The Tr-NOESY spectra were acquired at a mixing time of 150 ms.

spectra, suggesting overall flexible conformations of YW12 in the unbound state (data not shown).

Additions of low concentrations of LPS into a solution of YW12 result in concentration-dependent broadening of many proton resonances without any significant change in chemical shifts suggesting a first or intermediate exchange between free and LPS bound YW12 at NMR time scale (Figure 4A). At higher concentrations of LPS (peptide/LPS ~1:1), the peptide/LPS complex showed a strong tendency for precipitation, preventing structural studies under such conditions (data not shown). The LPS-induced broadening of peptide resonances prompted us to examine the conformation of the LPS bound form of YW12 by using Tr-NOE measurements. Figure 4B (right panel) shows the 2D Tr-NOESY spectrum of YW12 peptide, correlating low-field proton resonances (6.7−8.5 ppm) at the ω_2 dimension with the aliphatic backbone and side chain proton resonances (4.7−0.68 ppm) at the ω_1 dimension. There is a remarkable improvement of the NOESY spectrum in terms of the number and intensity of NOE cross-peaks, indicating ordering of the conformation of the peptide in complex with LPS. The most downfield shifted N$^{\varepsilon}$H proton of W4 shows a number of well-resolved

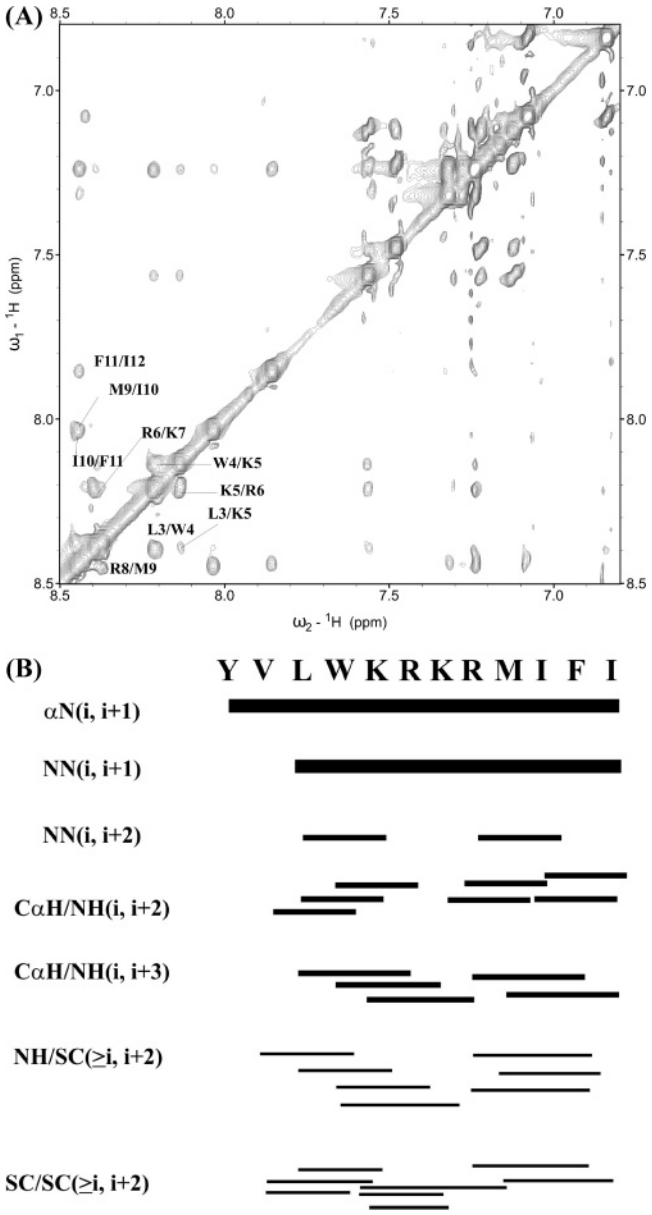

FIGURE 5: (Panel A) Two-dimensional ^{1}H-^{1}H Tr-NOESY spectrum showing NOEs between amide protons and aromatic protons. Only NOEs among amide protons are labeled. The Tr-NOESY spectra were acquired at a mixing time of 150 ms. (Panel B) Bar diagram summarizing Tr-NOEs observed for the YW12 peptide in complex with LPS. The thickness of the bar is proportional to NOE intensity.

NOE cross-peaks with the backbone and alkyl side chain proton resonances from other residues (Figure 4B, left panel). The large molecular weight aggregates of LPS formed at a very low concentration (14 μg/mL) (*36*) permit the observation of Tr-NOE cross-peaks from the bound peptide ligands with dissociation constants (K_d) in the micromolar range (*37*−*39*). Analyses of Tr-NOE spectra reveal that most of the backbone/backbone NOEs, that is, C$^\alpha$H/HN or HN/HN, are sequential (i to $i + 1$) or medium range (i to $i + 2$, $i + 3$) in nature (Figure 5A and B). Apart from these, a large number of sequential and medium-range side chain/side chain and side chain/backbone NOEs could be unambiguously assigned. These NOEs involve the aromatic side chain protons of residues Y1, W4, and F11 with the aliphatic side chain protons of residues V2, L3, M9, I10, and I11 (Figure 5B). Few long-range NOEs (i to $i + 5$) could be unambiguously assigned between aromatic ring protons of W4 with the C$^\epsilon$H$_3$ group, resonating at 2.06 ppm, of the M9 residue (Figure 5B).

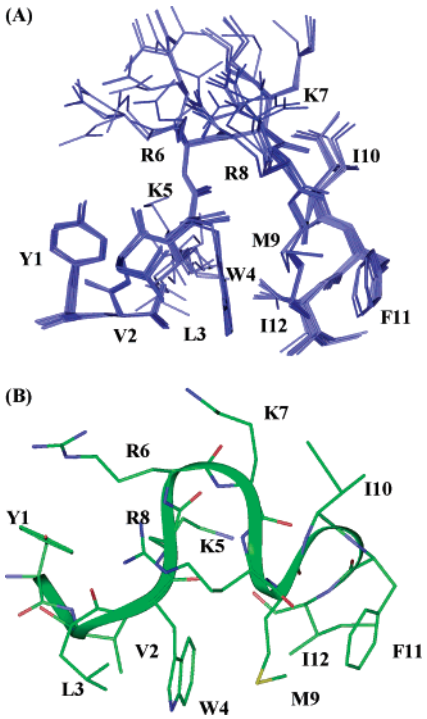

FIGURE 6: (Panel A) Superposition of all heavy atoms of 20 lowest energy structures and (Panel B) the orientation of side chains of a representative structure of the YW12 peptide while bound to LPS. The side chains are depicted as sticks, whereas the backbone is presented as a ribbon.

Table 1: Summary of Structural Statistics for the 20 Final Structures of LPS Bound YW12

distance restraints	
total	120
intraresidue ($i - j = 0$)	0
sequential ($\|i - j\| = 1$)	57
medium-range ($2 \leq \|i - j\| \leq 4$)	59
long-range ($\|i - j\| \geq 5$)	4
angular restraints (Φ)	11
distance restraints violations	
number of violations	12
average violation	≤0.10 Å
maximum violation	≤0.30 Å
deviation from mean structure (for all residues)	
backbone (C$^\alpha$, C′, and N)	0.2 Å
heavy atoms	1.3 Å
Ramachandran plot for the mean structure	
% residues in the most favorable and additionally allowed region	95
% residues in the generously allowed region	5
% residues in the disallowed region	0

Structure of YW12 Bound to Lipopolysaccharide. A high-resolution solution structure of YW12 in complex with LPS has been obtained by using ∼120 Tr-NOE driven distance restraints (Table 1). The backbone dihedral angle ϕ was generously relaxed for all of the residues to sample the allowed region of the Ramachandran map (see Materials and Methods). No other distance or angular constraints were taken into account during computations. Figure 6A shows the superposition of all heavy atoms and backbone atoms (C$^\alpha$, N, and C′) of the 20 lowest energy structures of YW12. The LPS bound conformation of YW12 is well defined with a backbone rmsd of 0.2 Å. The rmsd value for all heavy

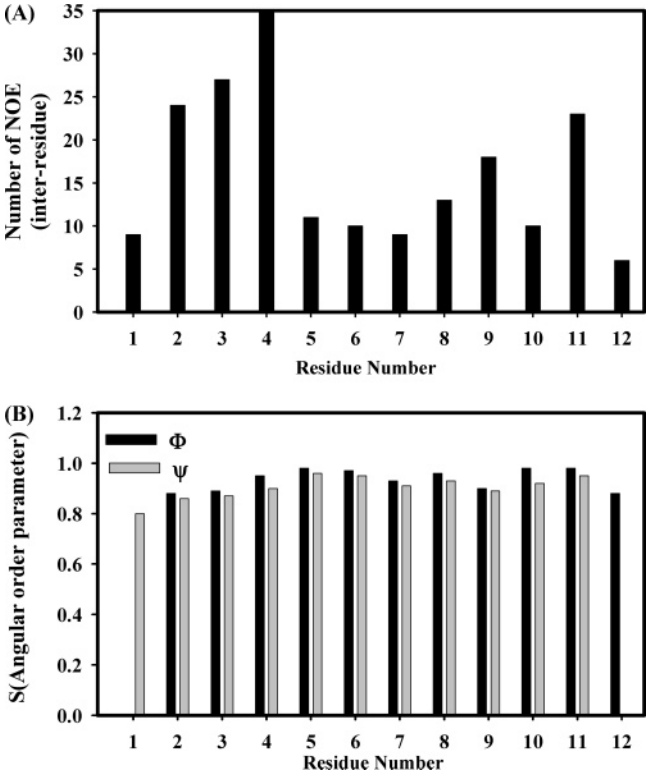

FIGURE 7: (Panel A) Bar diagram showing the number of inter-residue Tr-NOEs observed per residue of YW12 while bound to LPS. (Panel B) Bar diagram showing the calculated angular order parameter (*S*) for the backbone dihedral angles (ϕ, ψ) of each residue obtained from the 20 lowest energy structures of YW12 in the presence of LPS.

atoms is also restricted to ~1.2 Å (Table 1). The side chain orientations of most of the hydrophobic and aromatic residues, in particular residues Y1, V2, L3, W4, M9, and F11, are very well defined (Figure 6A). However, the side chains of the four positive charged residues (K5-R6-K7-R8) appear to be sampling a somewhat larger conformational space (Figure 6A). This could be attributed to lack of sufficient NOE constraints for the side chains of the central charged segment. Figure 6B represents the disposition of side chains of LPS bound YW12. Strikingly, most of the hydrophobic and aromatic residues segregate on to one side, whereas the centrally placed charged residues are directed at the opposite face of the molecule, essentially giving rise to an amphipathic structure. The hydrophobic core of LPS bound YW12 is defined by intimate contacts among the side chain of residues V2, L3, and W4 from the N-terminus and the side chain of residues, M9, F11, and I12, from the C-terminus of YW12 (Figure 6B). The mutual packing of the side chains of residue W4 and residue M9 plausibly play an important role connecting the N-terminus hydrophobic cluster with the C-terminus one. The side chains of residues Y1 and I10 lay at the top of the hydrophobic surface (Figure 6B). An overall well-defined structure of YW12 in complex with LPS results from a large number of inter-residue NOE contacts observed for the nonpolar and aromatic residues (Figure 7A). In particular, W4 shows as many as 36 inter-residue NOEs followed by residues V2, L3, F11, and M9 (Figure 7A). Figure 7B shows the angular order parameter (*S*) of backbone dihedral angles (ϕ, ψ) of each residue of YW12. An *S* value (see Material and Methods) close to 1 for most of the residues indicates a well-defined backbone conformation of the peptide in complex with LPS.

The backbone of LPS bound YW12 does not adopt any common secondary structures such as the α-helix or β-sheet. The N-terminus half, residues V2−R6, of YW12 rather shows a loop or extended conformations; however, two consecutive β-turns are observed at the C-terminus encompassing residues K7−I12 (Figure 6B). These type III β-turns are defined by residues K7-R8-M9-I10 and M9-I10-F11-I12. The formation of β-turns is supported by the diagnostic backbone NOE patterns typified by strong intensity HN/HN (i to $i + 1$) NOEs and medium intensity CαH/HN (i to $i + 2$) NOEs (*34*) (Figure 5). In addition, a relatively weak NOE is observed between the amide protons of residues R8 and I10, authenticating nucleation of a β-turn centering residues R8 and M9 at the C-terminus of YW12 in complex with LPS. Similar HN/HN (i to $i + 2$) NOEs could not be detected between residues M9 and F11 for the second β-turn because of spectral overlap. Interestingly, in all of the calculated structures, the amide protons of residue I10 and residue I12 have been found to be in close proximity (2.2−2.5 Å) to the carbonyl oxygen of residues K7 and M9, respectively, indicating the possibility of hydrogen bond formation (data not shown). A long-range hydrogen bond interaction has also been detected in some calculated structures between the amide proton of residue M9 and the carbonyl oxygen of residue W4 (data not shown).

A Tr-NOE derived structure of YW12 was docked on to LPS to obtain a model of the peptide/LPS complex (Figure 8A and B). In the complex, YW12 is found to be aligned parallel to the plane of the long axis of LPS. The centrally located basic residues appear to form a number of salt bridges and hydrogen bond interactions primarily with the phosphate groups attached to the two glucosamines of the lipid A moiety of LPS (Figure 8A). In particular, the ϵ-amino group of residue K5 is in close proximity to the phosphate group located at the $O_{4'}$ position of glucosamine II, whereas the phosphate at the O_1 position of glucosamine I can potentially form ionic hydrogen bonds with residues R6 and K7. The centrally located guanidinium group of R6 is so positioned as to be able to form string ionic H-bond interactions with either phosphate group of lipid A (Figure 8A). Close packing is also observed between aromatic and nonpolar residues, in particular M9, I10, F11, and I12, from the C-terminal half of the peptide with the acyl chains of the LPS molecule (Figure 8B). The indole side chain of W4 is found to be positioned at the interface between the polar and hydrophobic layer of LPS (Figure 8B).

Localization of YW12 in Micelles. The interactions of the peptide with various lipid micelles including SDS, POPG, LPS, and DPC were investigated utilizing the intrinsic tryptophan fluorescence of YW12. The tryptophan fluorescence of the free peptide shows an emission maximum (λ_{max}) at ~355 nm, implying its full exposure to the aqueous environment. In negatively charged micelles, SDS, LPS, and POPG, there is a dramatic blue shift (shift toward shorter wavelength) of the λ_{max} of tryptophan, indicating incorporation of the peptide into the hydrophobic milieu of the micelles (Figure 9A) (*40*). The extent of blue shift is higher for SDS micelles with an enhancement of fluorescence intensity followed by LPS and POPG (Table 2). Very interestingly, there is no significant change in the λ_{max} of tryptophan

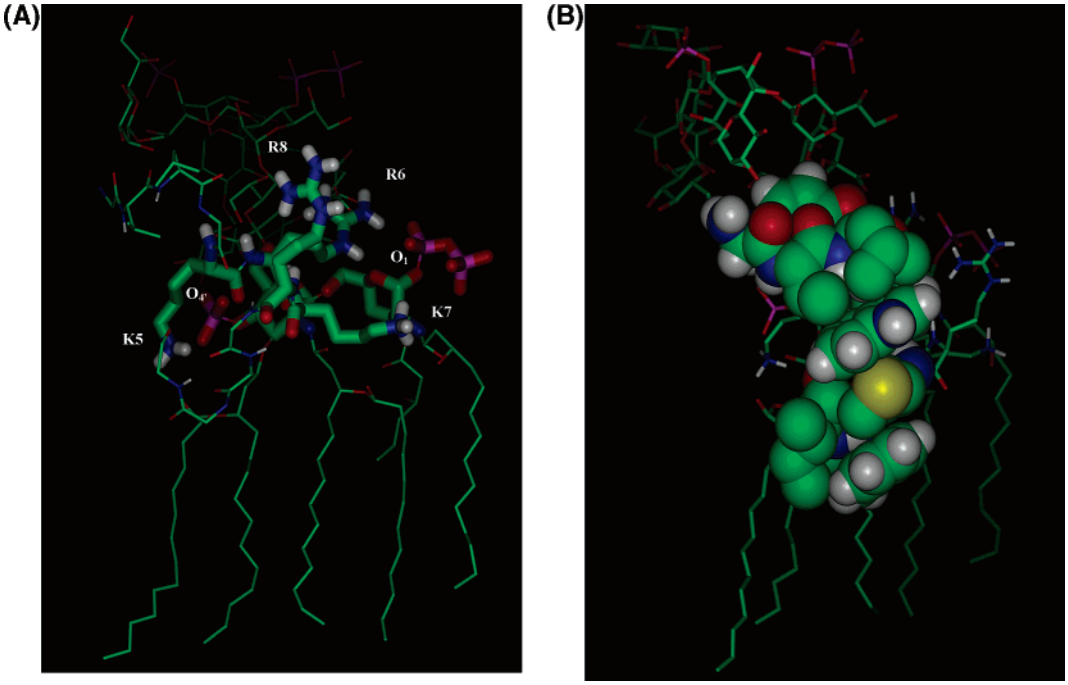

FIGURE 8: Model of the YW12−LPS complex. (Panel A) Plausible ionic and hydrogen bond interactions between the positively charged amino acid residues (represented by a thick stick) of YW12 and the negatively charged phosphate groups (represented by a thick stick) of the lipid A moiety of LPS. (Panel B) Space-filling representation of the hydrophobic residues of YW12 in the LPS−peptide complex.

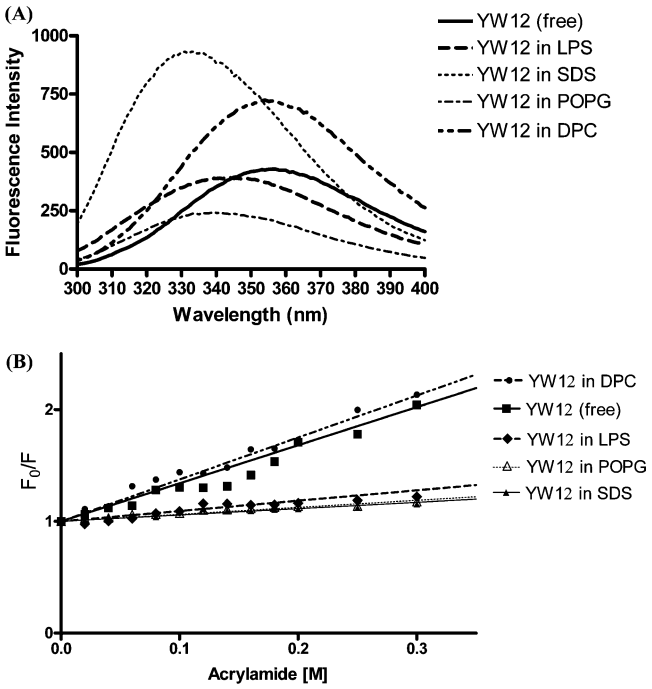

FIGURE 9: (Panel A) Tryptophan fluorescence emission spectra of the YW12 peptide in 10 mM sodium phosphate buffer at pH 6.0 and in 10 mM sodium phosphate buffer solutions at pH 6.0 containing LPS (40 μg/mL), POPG (1.2 mM), SDS (10 mM), and DPC (1.2 mM) micelles. (Panel B) Fluorescence quenching of the YW12 peptide by acrylamide in 10 mM sodium phosphate buffer at pH 6.0 and in 10 mM sodium phosphate buffer solutions at pH 6.0 containing LPS (40 μg/mL), POPG (1.2 mM), SDS (10 mM), and DPC (1.2 mM) micelles.

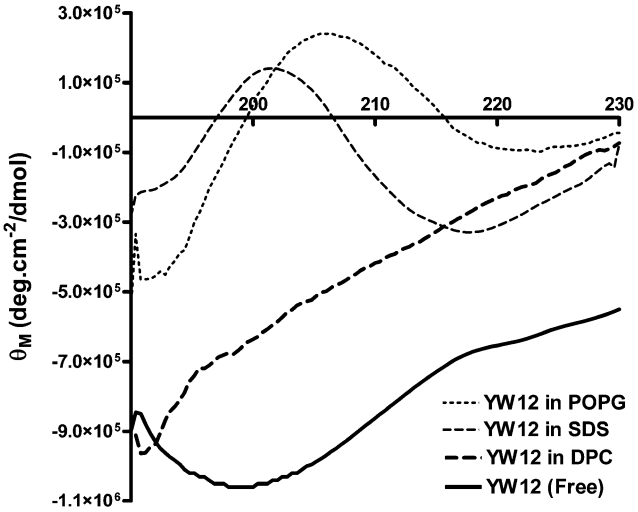

FIGURE 10: Far-UV CD spectra of YW12 in 10 mM sodium phosphate buffer solution at pH 6.0 and in 10 mM sodium phosphate buffer solutions at pH 6.0 containing POPG (1.2 mM), SDS (10 mM), and DPC (1.2 mM) micelles.

Table 2: Tryptophan Fluorescence Emission Maxima (λ_{max}) and Stern−Volmer Quenching Constants (K_{sv}) of the YW12 Peptide in DPC, LPS, POPG, and SDS Micelles

micelle types	λ_{max}	acrylamide quenching	iodide quenching
YW12−buffer	353.00	3.4 ± 0.14	9.3 ± 0.25
YW12−DPC	354.00	3.8 ± 0.072	25 ± 0.46
YW12−LPS	343.07	0.93 ± 0.057	6.6 ± 0.37
YW12−POPG	339.07	0.63 ± 0.023	4.7 ± 0.38
YW12−SDS	333.07	0.57 ± 0.032	3.3 ± 0.23

fluorescence in zwitterionic micelle DPC, although an enhancement of fluorescence intensity is observed (Figure 9A), possibly indicating a weak interaction that is restricted only at the surface of the micelles. Tryptophan fluorescence quenching by acrylamide or potassium iodide demonstrates that the tryptophan residue is significantly protected from quenching in negatively charged micelles (Figure 9B and Table 2).

Secondary Structure of YW12 in Micelles. In aqueous solution, the far-UV CD spectrum of free peptide is

characterized by a broad band at ~200 nm (Figure 10), the typical signature for random coil-like conformations (*41*). This observation is in accordance with NMR and fluorescence results suggesting that uncomplexed YW12 does not adopt any regular secondary structures. There is a dramatic change in the CD spectrum of YW12 both in the presence of SDS and POPG, signaling structural changes upon binding with the negatively charged micelles (Figure 10). The negative CD ellipticity ~200 nm observed for the free peptide disappeared with a concomitant rise of a positive CD band centering at ~202 nm and at ~207 nm in SDS and POPG, respectively. Apart from the positive band, the CD spectra of YW12 are also characterized by a negative band at ~220 nm in SDS and at ~218 nm in POPG (Figure 10). However, the CD spectrum of YW12 in DPC micelles remains very similar to the one observed for the free peptide, suggesting the absence of structural changes in the zwitterionic micelle (Figure 10). Although the presence of positive band either at ~207 nm or at ~202 nm in SDS and POPG, respectively, could possibly suggest β-turns or β-type conformations, a detailed assignment of the secondary structures of the YW12 peptide in complex with SDS or POPG from CD experiments was difficult because of the significant contribution to the far-UV CD spectra from the aromatic residues (*42*).

DISCUSSION

Neutralization of LPS Toxicity by the YW12 Peptide. We have demonstrated that YW12 binds to LPS and neutralizes its toxicity, although the LPS neutralization activity of YW12 is modest (IC_{50} ~10 μM) compared to that of polymyxin B (IC_{50} ~1.23 μM), the gold standard sequestrant of LPS (*14*). The high LPS neutralization activity of polymyxin B is strictly conferred by its cyclic structure and a long acyl group attached to the amino terminal end (*22*). However, these structural features of polymyxin B also render the antibiotic toxic to humans. Future cycles of design and evaluation will include the parallel evaluation of affinity, activity, and toxicity.

Amphipathic Structure of YW12 in Complex with LPS. The free peptide predominantly adopts random conformations in solution as suggested by NMR parameters, far-UV CD, and intrinsic tryptophan fluorescence. As a complex with LPS, YW12 folds into a unique amphipathic structure with two distinct surfaces of opposite polarity. The hydrophobic surface of the LPS bound structure of YW12 is defined by the intimate packing among the side chains of nonpolar and aromatic residues, whereas the positively charged residues are segregated on to the other surface. In the docked structure of the LPS/YW12 complex, both surfaces are involved in the stabilization of the complex. A part of the hydrophobic core structure, particularly the C-terminal segment, of YW12 is engaged in interactions with the acyl chains of LPS, whereas the four positively charged residues appear to participate in the formation of salt bridges with the phosphate groups of the lipid A moiety of LPS. Interestingly, the parallel orientation of YW12 along the surface of LPS seems to mimic the interaction of LPS with FhuA (*29*). This is in contrast to the structure of polymyxin B in which we and others have demonstrated a different binding mode for polymyxin B (*37*, *38*) and polymyxin E (*38*) on to lipid A. The seven member cyclic structure of polymyxin has been found to be in an orthogonal orientation with the long axis of lipid A, whereas the linear portion of polymyxin containing the methyl-octanoyl chain remains coaxial with the acyl chains of lipid A (*37*). The model complex of YW12 and LPS presented here could be of further use in developing high-affinity LPS inhibitors. An alanine scan of the C-terminus hydrophobic residues of YW12 will reveal those interactions that significantly contribute to the binding energy of the complex. A structure−activity study on these residues being iteratively replaced with aliphatic residues or long chain acyl groups to optimize hydrophobic interactions will likely be instructive.

Table 3: Comparison of the Quality, in terms of rmsd, of Structures of LPS Bound Peptides Derived from Tr-NOE with Some Antimicrobial Peptides of Similar Length Determined by Conventional NMR Methods

peptide	length	NMR method	micelle	rmsd[a] (Å)	reference
YW12	12-linear	Tr-NOE	LPS	1.2	this study
LALF	14-cyclic	Tr-NOE	LPS	2.17	*44*
LF11	11-linear	Tr-NOE	LPS	1.25	*39*
LBP	14-linear	Tr-NOE	LPS	1.71	*45*
indolicidin	13-linear	conventional	SDS	1.52	*47*
indolicidin	13-linear	conventional	DPC	0.98	*47*
tritrpticin	13-linear	conventional	SDS	0.77	*46*

[a] The rmsd values quoted here are only for the well-structured region of the peptides.

The solution structures of membrane active antimicrobial peptides are traditionally obtained by using standard the 2D NMR method, whereby peptides are stably bound to SDS or DPC micelles (*43*). However, similar structural studies of peptides in complex with LPS have not been successful, presumably due to the heterogeneous nature of LPS aggregates and the strong propensity for precipitation of the LPS/peptide complex (*23*). The Tr-NOE method has met with notable success in determining LPS bound conformations of naturally occurring antimicrobial peptides including polymyxin B (*37*, *38*) and few peptide fragments derived from LPS binding proteins including LALF (*44*), LBP (*45*), and lactoferrin (*39*). The quality of Tr-NOE generated structures of LPS bound peptides appears to be comparable to the quality of those determined by conventional NMR methods in detergent micelles (Table 3). The amphipathic structure adopted by the YW12 peptide in the context of LPS has frequently been observed for naturally occurring antimicrobial peptides in model membranes (*46*−*51*). The formation of an amphipathic structure at the membrane−water interface has been thought to be a pre-requisite for the activity of many of these antimicrobial peptides (*35*, *52*−*54*). The interaction and neutralization of LPS toxicity by the YW12 peptide may indeed also rely on its ability to adopt an amphipathic structure in the context of LPS.

Micelle Selective Interactions of the Peptide. The binding of the YW12 peptide with negatively charged micelles, SDS and POPG, and zwitterionic micelles, DPC, has been probed in order to investigate whether peptide can discriminate among different types of membranes. The bacterial membrane is rich in negatively charged lipids, whereas the cell membrane of eukaryotes is predominantly zwitterionic in nature (*54*). Our results demonstrate that the designed peptide, YW12, interacts strongly with the negatively charged micelles as suggested by limited quenching of tryptophan

fluorescence intensity along with the large blue shift in the emission maximum of tryptophan fluorescence (Figure 9). The interactions of the negatively charged micelles with the peptide also caused a dramatic structural transition from random conformations in a free state to β-turns or β-sheet-like structures (Figure 10). On the contrary, the CD spectra of YW12 suggest that the peptide does not undergo any conformational transitions in the presence of DPC micelles (Figure 10). The inability of the peptide to penetrate DPC micelles is clearly evidenced by the high collisional quenching coefficients of tryptophan fluorescence intensity, which is similar to that of the free peptide (Figure 9). Collectively, these results suggest that the designed peptide, YW12, may discriminate between bacterial and mammalian cell types. Further studies are being undertaken to obtain a clear picture of this particular property of the peptide.

SUPPORTING INFORMATION AVAILABLE

NOE build up curves of the YW12 peptide in complex with LPS and the atomic coordinates of the YW12/LPS complex. This material is available free of charge via the Internet at http://pubs.acs.org.

REFERENCES

1. Raetz, C. R. H., and Whitfield, C. (2002) Lipopolysaccharide endotoxins, *Annu. Rev. Biochem. 71*, 635−700.
2. Rietschel, E. T., Kirikae, T., Schade, F. U., Mamat, U., Schmidt, G., Loppnow, H., Ulmer, A. J., Zahringer, U., Seydel, U., Di Padova, F., Schreier, M., and Brade, H. (1994) Bacterial endotoxin: molecular relationships of structure to activity and function, *FASEB J. 8*, 217−225.
3. Hancock, R. E., and Scott, M. G. (2000) The role of antimicrobial peptides in animal defenses, *Proc. Natl. Acad. Sci. U.S.A. 97*, 8856−8861.
4. Dinarello, C. A. (1996) Cytokines as mediators in the pathogenesis of septic shock, *Curr. Top. Microbiol. Immunol. 216*, 133−165.
5. Cohen, J. (2002) The immunopathogenesis of sepsis, *Nature 420*, 885−891.
6. Zhang, F. X., Krisching, C. J., Mancinelli, R., Xu, X. P., Jin, Y., Faure, E., Mantovani, A., Rothe, M., Muzio, M., and Arditi, M. (1999) Bacterial lipopolysaccharide activates nuclear factor-kappaB through interleukin-1 signaling mediators in cultured human dermal endothelial cells and mononuclear phagocytes, *J. Biol. Chem. 274*, 7611−7614.
7. Fink, P. F. (1990) In *Sepsis Syndrome. Handbook of Critical Care* (Berk, J. L., and Sampliner, J. E., Eds.), Little Brown and Co.: Boston.
8. Hardaway, R. M. (2000) Traumatic shock alias post-trauma critical illness, *Am. Surg. 66*, 22−29.
9. Schumann, R. R., Leong, S. R., Flaggs, G. W., Gray, P. W., Wright, S. D., Mathison, J. C., Tobias, P. S., and Ulevitch, R. J. (1990) Structure and function of lipopolysaccharide binding protein, *Science 249*, 1429−1431.
10. Wright, S. D., Ramos, R. A., Tobias, P. S., Ulevitch, R. J., and Mathison, J. C. (1990) CD14, a receptor for complexes of lipopolysaccharide (LPS) and LPS binding protein, *Science 249*, 1431−1433.
11. Poltorak, A., He, X., Smirnova, I., Liu, M. Y., Van Huffet, C., Du, X., Birdwell, D., Alejos, E., Silva, M., Galanos, C., Freudenberg, M., Ricciardi-Castagnoli, P., Layton, B., and Beutler, B. (1998) Defective LPS signaling in C3H/HeJ and C57BL/10ScCr mice: mutations in Tlr4 gene, *Science 282*, 2085−2088.
12. Lee, H. K., Dunzendorfer, S., and Tobias, P. S. (2004) Cytoplasmic domain-mediated dimerizations of toll-like receptor 4 observed by beta-lactamase enzyme fragment complementation, *J. Biol. Chem. 279*, 10564−10574.
13. Martin, G. S., Mannino, D. M., Eaton, S., and Moss, M. (2003) The epidemiology of sepsis in the United States from 1979 through 2000, *N. Engl. J. Med. 348*, 1546−1554.
14. David, S. A. (2001) Towards a rational development of anti-ednotoxin agents: novel approaches to sequestration of bacterial endotoxins with small molecules, *J. Mol. Recognit. 14*, 370−387.
15. Boman, H. G. (1995) Peptide antibiotics and their role in innate immunity, *Annu. Rev. Immunol. 13*, 61−92.
16. Scott, M. G., Yan, H., and Hancock, R. E. (1999) Biological properties of structurally related alpha-helical cationic antimicrobial peptides, *Infect. Immun. 67*, 2005−2009.
17. David, S. A., Awasthi, S. K., and Balaram, P. (2000) The role of polar and facial amphipathic character in determining lipopolysaccharide-binding properties in synthetic cationic peptides, *J. Endotoxin Res. 6*, 249−256.
18. Muhle, S. A., and Tam, J. P. (2001) Design of Gram-negative selective antimicrobial peptides, *Biochemistry 40*, 5777−5785.
19. Scott, M. G., Vreugdenhil, A. C., Buurman, W. A., Hancock, R. E., and Gold, M. R. (2000) Cutting edge: cationic antimicrobial peptides block the binding of lipopolysaccharide (LPS) to LPS binding protein, *J. Immunol. 164*, 549−553.
20. Jerala, R., and Porro, M. (2004) Endotoxin neutralizing peptides, *Curr. Top. Med. Chem. 4*, 1173−1184.
21. Tan, N. G., NG, M., Yau, Y., Chong, P. K., Ho. B., and Ding, J. L. (2000) Definition of endotoxin binding sites in horseshoe crab factor C recombinant sushi proteins and neutralization of endotoxin by sushi peptides, *FASEB, J. 14*, 1801−1813.
22. Rustici, A., Velucchi, M., Faggioni, R., Sironi, M., Ghezzi, P., Quataert, S., Green, B., and Porro, M. (1993) Molecular mapping and detoxification of the lipid A binding site by synthetic peptides, *Science 259*, 361−365.
23. Pristovsek, P., and Kidric, J. (2004) The search for molecular determinants of LPS inhibition by proteins and peptides, *Curr. Top. Med. Chem. 4*, 1185−1201.
24. Clore, G. M., and Gronenborn, A. M. (1982) Theory of the time dependent transferred nuclear Overhauser effect: applications to ligand protein complexes in solution, *J. Magn. Reson. 48*, 402−417.
25. Post, C. B. (2003) Exchange-transferred NOE spectroscopy and bound ligand structure determination, *Curr. Opin. Struct. Biol. 13*, 581−588.
26. Guntert, P., Mumenthaler, C., and Wüthrich, K. (1997) Torsion angle dynamics for NMR structure calculation with the new program DYANA, *J. Mol. Biol. 273*, 283−298.
27. Detlefsen, D. J., Thanabal, V., Pecoraro, V. L., and Wagner, G. (1991) Solution structure of Fe(II) cytochrome c551 from *Pseudomonas aeruginosa* as determined by two-dimensional ^{1}H NMR, *Biochemistry 31*, 11973−11977.
28. Morris, G. M., Goodsell, D. S., Halliday, R. S., Huey, R., Hart, W. E., Belew, R. K., and Olson, A. J. (1998). Automated docking using a Lamarckian genetic algorithm and an empirical binding free energy function, *J. Comput. Chem. 19*, 1639−1662.
29. Ferguson, A. D., Hofmann, E., Coulton, J. W., Diederichs, K, and Welte, W. (1998) Siderophore-mediated iron transport: crystal structure of FhuA with bound lipopolysaccharide, *Science 282*, 2215−2220.
30. Rietschel, E. T., Brade, H., Brade, L., Brandenburg, K., Schade, U. F., Seydel, U., Zahringer, U., Galanos, C., Luderitz, O., Westphal, O., Labischinski, H., Kusumoto, S., and Shiba, T. (1987) Lipid A, the endotoxic center of bacterial lipopolysaccharides: relation of chemical structure to biological activity, *Prog. Clin. Biol. Res. 231*, 25−53.
31. Ferguson, A. D., Welte, W., Hofmann, E., Linder, B., Holst, O., Coulton, J. W., and Diederichs, K. (2000) A conserved structural motif for lipopolysaccharide recognition by procaryotic and eucaryotic proteins, *Structure 8*, 585−592.
32. Schibli, D. J., Epand, R. F., Vogel, H. J., and Epand, R. M. (2002) Tryptophan-rich antimicrobial peptides: comparative properties and membrane interactions, *Biochem. Cell Biol. 80*, 667−677.
33. Bishop, C. M., Walkenhorst, W. F., and Wimley, W. C. (2001) Folding of β-sheets in membranes: specificity and promiscuity in peptide model systems, *J. Mol. Biol. 309*, 975−988.
34. Wüthrich, K. (1986) *NMR of Proteins and Nucleic Acids*, John Wiley & Sons, New York.
35. Zasloff, M. (2002) Antimicrobial peptides of multicellular organisms, *Nature 415*, 389−395.
36. Santos, N. C., Silva, A. C., Castanho, M. A., Martins-Silva, J., and Saldanha, C. (2003) Evaluation of lipopolysaccharide aggregation by light scattering spectroscopy, *ChemBioChem 4*, 96−100.

37. Bhattacharjya, S., David, S. A., Mathan, V. I., and Balaram, P. (1997) Polymyxin B nonapeptide: conformations in water and in lipopolysaccharide-bound state determined by two-dimensional NMR and molecular dynamics, *Biopolymers 41*, 251−265.
38. Pristovsek, P., and Kidric, J. (1999) Solution structure of polymyxins B and E and effect of binding to lipopolysaccharide: an NMR and molecular modeling study, *J. Med. Chem. 42*, 4604−4613.
39. Japelj, B., Pristovsek, P., Majerle, A., and Jerala, R. (2005) Structural origin of endotoxin neutralization and antimicrobial activity of a lactoferrin-based peptide, *J. Biol. Chem. 280*, 16955−16961.
40. Lakowicz, J. R. (1983) *Principles of Fluorescence Spectroscopy*, Plenum press, New York.
41. Adler, A. J., Greenfield, N. J., and Fasman, G. D. (1973) Circular dichroism and optical rotatory dispersion of proteins and polypeptide, *Methods Enzymol. 27*, 675−735.
42. Woody, R. W. (1994) Contributions of tryptophan side chains to the far-ultraviolet circular dichroism of proteins, *Eur. Biophys. J. 23*, 253−262.
43. Chan, D. I., Prenner, E. J., and Vogel, H. J. (2006) Tryptophan- and arginine-rich antimicrobial peptides: structures and mechanisms of action, *Biochim. Biophys. Acta 1758*, 1184−1202.
44. Pristovsek, P., Feher, K., Szilagyi, L., and Kidric, J. (2005) Structure of a synthetic fragment of the LALF protein when bound to lipopolysaccharide, *J. Med. Chem. 48*, 1666−1670.
45. Pristovsek, P., Simcic, S., Wraber, B., and Urleb, U. (2005) Structure of a synthetic fragment of the lipopolysaccharide (LPS) binding protein when bound to LPS and design of a peptidic LPS inhibitor, *J. Med. Chem. 48*, 7911−7914.
46. Schibli, D. J., Hwang, P. M., and Vogel, H. J. (1999) Structure of the antimicrobial peptide tritrpticin bound to micelles: a distinct membrane-bound peptide fold, *Biochemistry 38*, 16794−16755.
47. Rozek, A., Friedrich, C. L., and Hancock, R. E. (2000) Structure of the bovine antimicrobial peptide indolicidin bound to dodecylphosphocholine and sodium dodecyl sulfate micelles, *Biochemistry 39*, 15765−15774.
48. Inagaki, F., Shimada, I., Kawaguchi, K., Hirano, M., Terasawa, I., Ikura, T., and Go, N. (1989) Structure of melittin bound to perdeuterated dodecylphosphocholine micelles as studied by two-dimensional NMR and distance geometry calculations, *Biochemistry 28*, 5985−5991.
49. Wang, G., Li, Y., and Li, X. (2005) Correlation of three-dimensional structures with the antibacterial activity of a group of peptides designed based on a nontoxic bacterial membrane anchor, *J. Biol. Chem. 280*, 5803−5811.
50. Powers, J. P., Tan, A., Ramaoorthy, A., and Hancock, R. E. (2005) Solution structure and interaction of the antimicrobial polyphemusins with lipid membranes, *Biochemistry 44*, 15504−15513.
51. Jing, W., Demcoe, A. R., and Vogel, H. J. (2003) Conformation of a bactericidal domain of puroindoline a: structure and mechanism of action of a 13-residue antimicrobial peptide, *J. Bacteriol. 185*, 4938−4947.
52. Brogden, K. A. (2005) Antimicrobial peptides: pore formers or metabolic inhibitors in bacteria, *Nature 3*, 238−250.
53. Hwang, P. M., and Vogel, H. J. (1998) Structure-function relationships of antimicrobial peptides, *Biochem. Cell Biol. 76*, 235−246.
54. Matsuzaki, K. (1999) Why and how are peptides-lipid interactions utilized for self-defense? magainins and tachyplesins as archetypes, *Biochim. Biophys. Acta 1462*, 1−10.

BI6025159